Virus Research 270 (2019) 197644

Contents lists available at ScienceDirect

Virus Research

journal homepage: www.elsevier.com/locate/virusres

Short communication

Molecular variability of apple hammerhead viroid from Italian apple varieties supports the relevance *in vivo* of its branched conformation stabilized by a kissing loop interaction

Michela Chiumenti[a], Beatriz Navarro[a], Pasquale Venerito[b], Francesco Civita[c], Angelantonio Minafra[a,*], Francesco Di Serio[a,*]

[a] Istituto per la Protezione Sostenibile delle Piante (CNR), Bari, Italy
[b] Centro di Ricerca, Sperimentazione e Formazione in Agricoltura "Basile Caramia", Locorotondo, Italy
[c] SINAGRI – Università degli Studi di Bari "Aldo Moro", Bari, Italy

ARTICLE INFO

Keywords:
Hammerhead
Non-Coding RNA
Sequence variability
Secondary structure
Co-Variation
Stem-Loop

ABSTRACT

In the absence of protein-coding ability, viroid RNAs rely on direct interactions with host factors for their infectivity. RNA structural elements are likely involved in these interactions. Therefore, preservation of a structural element, despite the sequence variability existing between the variants of a viroid population, is considered a solid evidence of its relevant role *in vivo*. In this study, apple hammerhead viroid (AHVd) was first identified in the two apple cultivars 'Mela Rosa Guadagno' (MRG) and 'Agostinella' (AG), which are cultivated since long in Southern Italy, thus providing the first solid evidence of its presence in this country. Then, the natural variability of AHVd viroid populations infecting MRG and AG was studied. The sequence variants from the two Italian isolates shared only 82.1–87.7% sequence identity with those reported previously from other geographic areas, thus providing the possibility of exploring the impact of this sequence divergence on the proposed secondary structure. Interestingly, all the AHVd sequence variants considered in this study preserved a branched secondary structure stabilized by a kissing-loop interaction, resembling the conformation proposed previously for variants from other isolates. Indeed, most mutations did not modify the proposed conformation because they were co-variations, conversions of canonical into wobble base-pairs, or *vice versa*, as well as changes mapping at loops. Importantly, a cruciform structural element formed by four hairpins, one of which is implicated in the proposed kissing-loop interaction, was also preserved because several nucleotide changes actually resulted into two, three and up to five consecutive co-variations associated with other changes that did not affect the secondary structure. These data provide very strong evidence for the relevance *in vivo* of this cruciform structure which, together with kissing-loop interaction, likely contribute to further stabilizing the branched AHVd secondary structure.

The genome of viroids, the smallest infectious agents known so far, is composed of a tiny (250–400 nt), circular RNA that does not code for any protein (Diener, 2003; Flores et al., 2005; Gomez and Pallás, 2013; Palukaitis, 2014; Gago-Zachert, 2016). Therefore, the enzymatic functions and molecular machineries needed for viroid replication and trafficking in the infected plant are provided by host factors or by catalytic activities contained in the viroid RNA. On the one hand, self-cleavage mediated by hammerhead ribozymes observed in member of the family *Avsunviroidae* (Di Serio et al., 2018b) is a solid evidence that such an RNA-mediated enzymatic activity indeed exists in some viroids. On the other hand, the documented involvement of several host enzymes in the replication of viroids is also a good evidence that they are able to interact and redirect host enzymes (and other host factors) for their replication and movement within the plant (Flores et al., 2017). This capacity very likely depends on structural elements contained in the viroid RNAs that allow a direct interaction with the host factors needed for accomplishing the infectious cycle (Flores et al., 2012, 2015).

Viroids have the typical features of quasispecies (Codoñer et al., 2006), which means that the viroid population in a single host is composed of heterogeneous sequence variants slightly differing from each other. This is likely due to the errors introduced by the DNA-dependent RNA polymerases involved in viroid replication, which are forced to use RNA instead of their physiological DNA templates (Flores

* Corresponding authors.
E-mail addresses: angelantonio.minafra@ipsp.cnr.it (A. Minafra), francesco.diserio@ipsp.cnr.it (F. Di Serio).

https://doi.org/10.1016/j.virusres.2019.197644
Received 18 May 2019; Received in revised form 24 June 2019; Accepted 26 June 2019
Available online 27 June 2019
0168-1702/

et al., 2017), thus making viroids the biological entities with the highest mutation rate ever reported (Gago et al., 2009; López-Carrasco et al., 2017). Additional source of sequence variability derives from recombination events that have been also frequently documented in several viroid RNAs (Haseloff and Symons, 1982; Fadda et al., 2003). Sequence variability generated by the high mutation rate and recombination events is largely constrained by selection pressure, which strongly reduces the number of sequence variants able to efficiently replicate and spread in the host. Therefore, it is not surprising that the preservation of elements of secondary and tertiary structure, likely involved in replication, trafficking and disruption of plant defense mechanisms, has been reported as a major restraint in viroid evolution (Elena et al., 2009; Flores et al., 2012). In this respect, the identification in a viroid population of sequence variants with mutations that do not modify the proposed viroid conformation (such as co-variations, conversions of canonical into wobble base-pairs, or *vice versa*, and changes preserving kissing-loop interactions), is considered firm evidence for a relevant role *in vivo* of the proposed viroid structural elements (Flores et al., 2012).

In the last few years, several circular RNAs containing the typical structural features of viroids and viroid-like RNAs have been identified using high-throughput sequencing (HTS) technologies (Barba and Hadidi, 2017). To ascertain whether a circular RNA is a viroid, *i.e.* whether it is infectious and able to replicate in the absence of any helper virus, biological assays showing its autonomous replication and spread in the host plant are needed (Di Serio et al., 2018a). In the case of a small circular RNA containing hammerhead ribozymes in both polarity strands that has been identified by HTS in apple trees in China (Zhang et al., 2014), this evidence has been recently provided (Serra et al., 2018). Bioassays, performed inoculating in apple plants head-to-tail full-length dimeric constructs of the viroid-like RNA, have conclusively shown that it is actually a viroid, now called apple hammerhead viroid (AHVd, Serra et al., 2018). In the same study, based on sequence variability of viroid populations and *in silico* modeling, branched conformations have been proposed for the AHVd circular monomeric forms of (+) and (-) polarity. By convention, the (+) polarity is assigned to the viroid RNA strand that accumulates at higher level *in vivo* and the (-) polarity to the complementary strand generated as a replication intermediate. Interestingly, the (+), but not the (-) strand of AHVd was proposed to be stabilized by a kissing loop-interaction (Serra et al., 2018), a situation resembling that reported in peach latent mosaic viroid (PLMVd; Hernández and Flores, 1992) by Bussière et al. (2000) and chrysanthemum chlorotic mottle viroid (CChMVd) (Gago et al., 2005), which have been classified in the genus *Pelamoviroid*, family *Avsunviroidae* (Navarro and Flores, 1997). Due to these structural features, it has been proposed to consider AHVd as a novel species in the genus *Pelamoviroid* (Serra et al., 2018). Members of this family replicate and accumulate in the chloroplasts thus largely differing from members of the family *Pospiviroidae* that replicate and accumulate in the nucleus (Di Serio et al., 2017).

AHVd has been reported in several apple cultivars in China (Zhang et al., 2014) and in the apple cultivar Pacific Gala in Canada (Messmer et al., 2017) and, more recently, in the apple cultivar 'Honeycrisp' in the USA (Szostek et al., 2018). The possible presence of this viroid in Japan, New Zealand, Italy and Spain has been inferred from the identification of AHVd sequences in plant material imported from these countries into the USA and maintained in a germplasm collection (Szostek et al., 2018). However, since the possibility that the plants in the germplasm collection could have become infected after their arrival cannot be excluded, and considering that AHVd has not been found in field trees in Europe, data supporting the presence in this continent of such infectious agent are not conclusive.

In the present study, the identification of AHVd in two local apple cultivars grown in southern Italy is reported, providing the first reliable evidence for the presence of this viroid in this country. Molecular data and phylogenetic analyses of AHVd sequence variants from the Italian isolates and comparisons with variants from isolates of other geographic origin provided solid support for the relevance *in vivo* of the overall secondary structure and the stabilizing kissing-loop proposed previously for AHVd (Serra et al., 2018). Additional structural elements conserved among variants differing in their primary structure, likely further stabilizing the AHVd branched conformation, have been also identified.

In the frame of a regional project aimed to rescue and characterize ancient fruit tree varieties from the Apulia region (Italy), samples were collected from native cultivars of fig, pear, apple, cherry, plum, almond, apricot and peach in the early summer (June) of 2016. The general sanitary status of these plants was checked by RT-PCR and ELISA for regulated viruses and viroids and a further analysis was performed using HTS. Starting from 250 mg of leaves and petioles from each plant, total RNAs were extracted according to a guanidine-based protocol (Foissac et al., 2001). These preparations were then enriched in dsRNAs by a double chromatography on non-ionic cellulose (CC41 Whatman), including an intermediate digestion step with DNase I and RNase A as reported by Marais et al. (2018). After quantification, dsRNAs from 12 plants of different species were normalized, pooled together, and used for generating a cDNA library, then submitted to a single-read 50 base-pair sequencing on an Illumina HiScan-SQ machine.

Reads were first screened for quality using the *fastx* toolkit (http://hannonlab.cshl.edu/fastx_toolkit/) and those with a quality score higher than 30 were assembled with the *Velvet* software (kmer 23) (Zerbino and Birney, 2008). All the contigs were searched either in Blastn (e-value threshold 10^{-6}) or Blastx (e-value threshold 10^{-4}). Blastn analyses revealed one contig, 301-nt long and covered by 65 non-redundant reads, that shared high sequence identity (91%) with the AHVd reference sequence (NC_028132). The sequence of such a contig corresponded to 69% of the complete genome of AHVd, thus suggesting that one or more plants included in the original pool were infected by this or a closely-related viroid. To identify the potentially infected host(s), all plants of the initial pool were tested by RT-PCR using *de novo* RNA extracts prepared according to Foissac et al. (2001). Reverse transcription was performed with random primers and M-MLV Reverse Transcriptase (200 U/L - Thermo Fisher Scientific, Waltham, MA USA). cDNAs were amplified using 1U of Dream *Taq* DNA polymerase (Thermo Fisher Scientific, Waltham, MA USA), and a set of adjacent primers of opposite polarity designed in the AHVd contig and covering the (+) hammerhead ribozyme domain (primer AHVd1-for: 5′-GTAGCCTAATAGACTACGACTTATGC-3′; primer AHVd1-rev: 5′-CTGATGAGTCCTTTTAGGACGAAACTT-3′); the amplification protocol included 35 cycles (95 °C for 30 s, 55 °C for 30 s, and 72 °C for 45 s, followed by a final elongation set at 72 °C for 7 min). Two samples, corresponding to the cultivars 'Mela Rosa Guadagno' (MRG) and 'Agostinella' (AG) grown in the municipalities of Troia and Orsara (Foggia, Italy), respectively, tested positive, while the other plant species and the apple cultivar "Limoncella", included in the HTS sequenced pool, tested negative. These data showed that AHVd was actually infecting two apple plants (approximatively 60 years old) belonging to different cultivars and from different locations about 20 Km distant from each other.

To characterize the viroid populations from the two isolates, the amplicons of the expected full-length size of the viroid (about 430 nt) generated by RT-PCR were cloned with the StrataClone PCR Cloning Kit (Agilent Technologies) and eight clones per sample sequenced in both directions. Based on the obtained sequences, a second pair of adjacent and complementary primers was designed in the AHVd (-) hammerhead ribozyme domain (primer AHVd2_for: 5′-CGTTCCAAGGACGAAACCGTTTCT-3′; primer AHVd2_rev: 5′-GACTCATCAGGAAGGCTAATAGCCT-3′) and used for extending the analyses of the viroid sequence variability to the region covered by the first set of primers (designed in the (+) hammerhead ribozyme), so that eight additional full-length viroid cDNAs from both MRG and AG samples were amplified, cloned and sequenced.

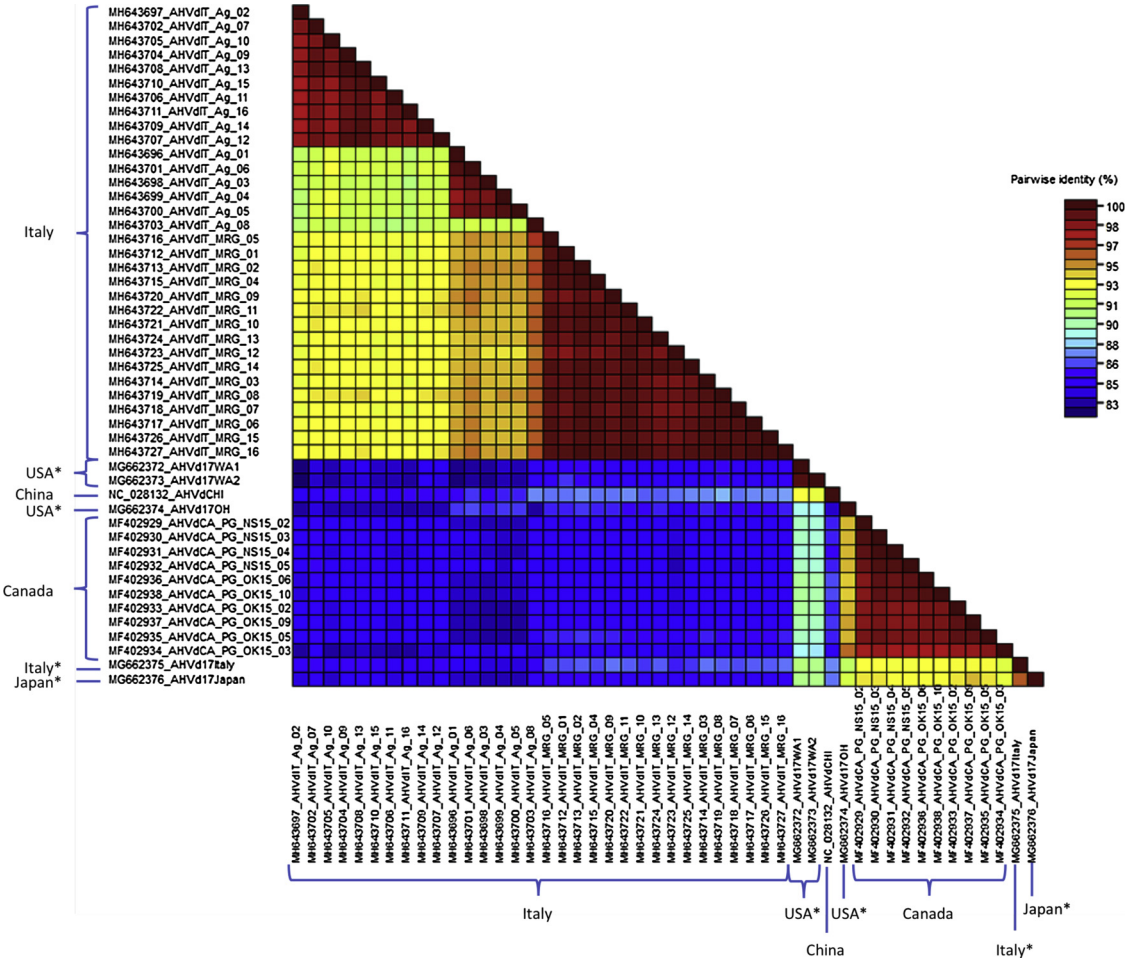

Fig. 1. Identity matrix generated by aligning AHVd sequence variants from AG and MRG isolates with those reported in literature. The geographic origin of the isolates is reported on the left and below the names of the variants. Asterisks denote isolates from germplasm collection.

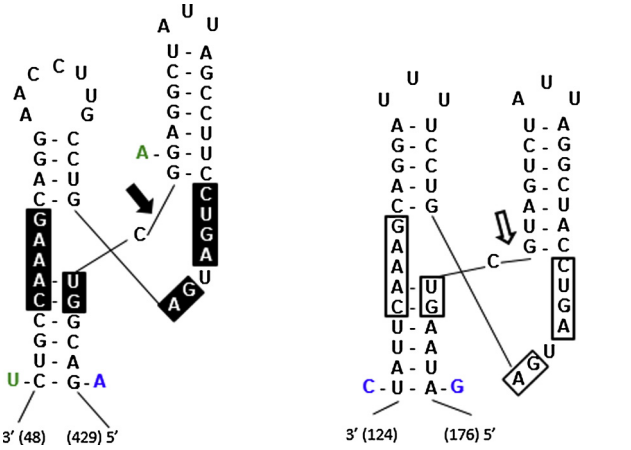

Fig. 2. AHVd hammerhead structures of the reference MRG sequence variant AHVd-IT_MRG_01 (MH643712). Mutations found in AG variants are reported in blue. Mutations found in variants from both AG and MRG isolates are indicated in green. To exclude changes potentially induced by the polymerase during the RT-PCR amplification step, only mutation found in more than one clone were reported. Arrows indicate self-cleavage sites, the nucleotide residues conserved in most natural hammerhead structures are boxed. Closed and open symbols refer to (+) and (-) polarities, respectively. The same numberings are used for the plus and minus polarities.

Multiple alignments and sequence identity matrices of the cloned sequences, generated by ClustalW (Hall, 2001; Thompson et al., 2003) and SDTv1.2 (Muhire et al., 2014), showed that AHVd populations from MRG and AG isolates are composed of sequence variants slightly differing from each other (Fig. S1 and S2). Composed of viroid variants sharing 98.4–99.8% sequence identity with each other, the viroid population from MRG isolate showed lower internal variability than that of the AG isolate, in which the sequence identity among AHVd variants ranged from 90.4 to 99.8% (Fig. S1 and S2). Moreover, the variants from both Italian cultivars largely differed from those previously reported in literature from China, Canada and, more recently, from the USA (sequence identity 82,1–87,7%, Fig. 1 and Fig. S3), with most of the nucleotide changes appearing not uniformly distributed along the aligned sequences, but located in short high variable regions (Fig. S3). Interestingly, polymorphic positions were also found in the hammerhead ribozyme domains of both polarity strands (Fig. S3), but the mutations did not impair the predicted base-pairing needed to form active ribozyme structures (Fig. 2).

In the phylogenetic tree generated in MEGA 7 by the neighbour-joining method (1000 bootstrap) including all the AHVd full-length sequences available in GenBank, the MRG and AG variants are clustered in two related clades, separated from all the other ones, thus supporting a closer relationship with each other than with all the other variants included in the analysis (Fig. 3). Moreover, with the exclusion of the isolates from a germplasm collection in the USA (Fig. 3), the phylogenetic relationships among the known AHVd variants almost completely mirror their geographic origin (Fig. 3). Altogether these data showed that AHVd has a higher sequence variability than thought before and

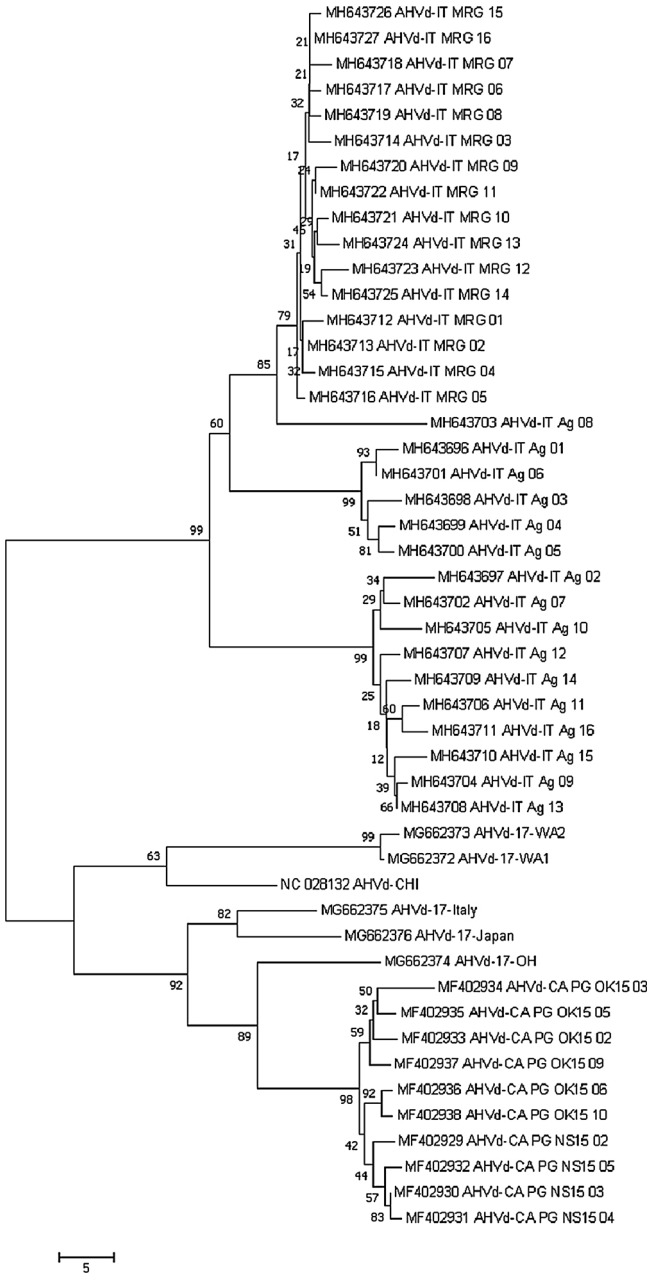

Fig. 3. Neighbor-joining phylogenetic tree generated using the AHVd variants from the apple trees (MRG and AG) grown in Italy and those reported in the literature. The geographic origin of each sequence variant is reported as follows: AHVd-IT, Italy; AHVd-CA, Canada; AHVd − CHI, China; AHVd-17 − OH, USA; AHVd-17-WA, USA. Statistical significance (in percentage) of nodes has been determined by bootstrap analysis after 1000 replicates and is indicated at each node.

allowed to further assess the effect of the observed nucleotide changes on the overall secondary structure and tertiary interactions proposed for this viroid.

Based on *in silico* and co-variation analyses, Serra et al. (2018) recently proposed branched secondary structures for both the (+) and the (-) polarity strands of AHVd. In the case of the (+) strand, the predicted conformation was composed of a rod-like domain that contains the conserved nucleotides forming the hammerhead ribozymes (hammerhead arm), and a highly branched domain, further stabilized by a kissing-loop interaction implicating four base pairing. By RNAfold [Vienna RNA package version 2.4.1 (Lorenz et al., 2011)] and some manual adjustments, a similar conformation was predicted for the (+) polarity strand of AHVd reference sequences from the MRG and AG isolates (GenBank MH643712-643727 and MH643696-64711, respectively) (Fig. 4). The sequence variability observed in the viroid populations, such as the branched conformation containing nine stem-loops (from SL-I to SL-IX), was almost completely preserved in all the AHVd variants from the Italian isolates because the changes with respect to the reference variant were prevalently co-variations, conversions of canonical into wobble base-pairs (or *vice versa*) or changes mapping at loops or unpaired regions (Fig. 4). In this respect, particularly interesting are three co-variations, two of which in consecutive positions, observed in the SL-II, which strongly support a relevance *in vivo* of this structural motif.

When the secondary structure predicted for the Italian AHVd variants (Fig. 4) was compared with that proposed by Serra et al. (2018), a similar general folding was observed, although the left terminal domain of the hammerhead arm (SL-I) was more stable in the former. In fact, due to nucleotide changes at several positions, a bulged sequence in the SL-I became paired in the Italian variants (Fig. 4, inset A). In contrast, the branched region was almost completely preserved in the two proposed secondary structures. However, in the Italian variants, due to a sequence rearrangement in both the interacting loops closing the SL-V and SL-VI, the potential kissing-loop structure predicted by Serra et al. (2018) (Fig. 4, inset B) was stabilized by three instead of four base pairs (Fig. 4). These findings are particularly relevant if one considers the high sequence variability between the Italian and the previously reported AHVd variants (Fig. S1, positions 297–407) in the region folding in the cruciform structural element formed by four hairpins (from SL-VI to SL-IX), one of which (SL-VI) is implicated in the proposed kissing-loop interaction (Fig. 4, inset B). In this region, the sequence variability between MRG or AG reference sequences and the Pacific Gala reference variant consisted of several mutations involving up to seven consecutive nucleotides. Notwithstanding these changes, the cruciform structure was preserved because the nucleotide changes in the hairpins were co-variations (two, three and up to five consecutive co-variations were counted in the SL-VII, SL-VII and SL-VI, forming the cruciform structure, respectively) or changes that converted canonical into wobble base pairs (Fig. 4, inset B). These concurrent mutations preserving the cruciform structural element, are very likely the outcome of important constraints derived from a still unknown functional role of this conserved region. In this respect, the results of our study provided an indirect but very strong evidence for the relevance *in vivo,* not only of the kissing-loop interaction highlighted previously (Serra et al., 2018), but also of the cruciform branched structure containing, and likely stabilizing, one of the hairpins contributing to the formation of this tertiary structural element. Interestingly, a similar cruciform structure containing a hairpin involved in a kissing-loop interaction was also present in the most stable conformation of CChMVd (Navarro and Flores, 1997), another member of the genus *Pelamoviroid.* Co-variations preserving this cruciform structural element were also reported in this case (Navarro and Flores, 1997; De la Peña et al., 1999; Gago et al., 2005), thus further extending to other pelamoviroids the possible biological relevance of such a cruciform structural element stabilized by the kissing-loop interaction.

To the best of our knowledge, this study provides the first evidence that AHVd is present in Europe. Considering that the infected cultivars were grown since long in Italy, the presence of AHVd in this continent could also be dated back to a long time ago. In addition, the sequence variability between the two Italian AHVd isolates and the previously reported sequence variants of this viroid provides solid evidence for the relevance *in vivo* of the overall branched conformation of this viroid stabilized by a kissing-loop interaction. Moreover, the co-variation analysis has allowed to identify in the SL-II and in the cruciform structure formed by four stem-loops (SL-VI to SL-IX), two additional structural elements with possible relevant roles for the viroid infectivity and/or fitness.

NOTE. When this article was being prepared for submission, another

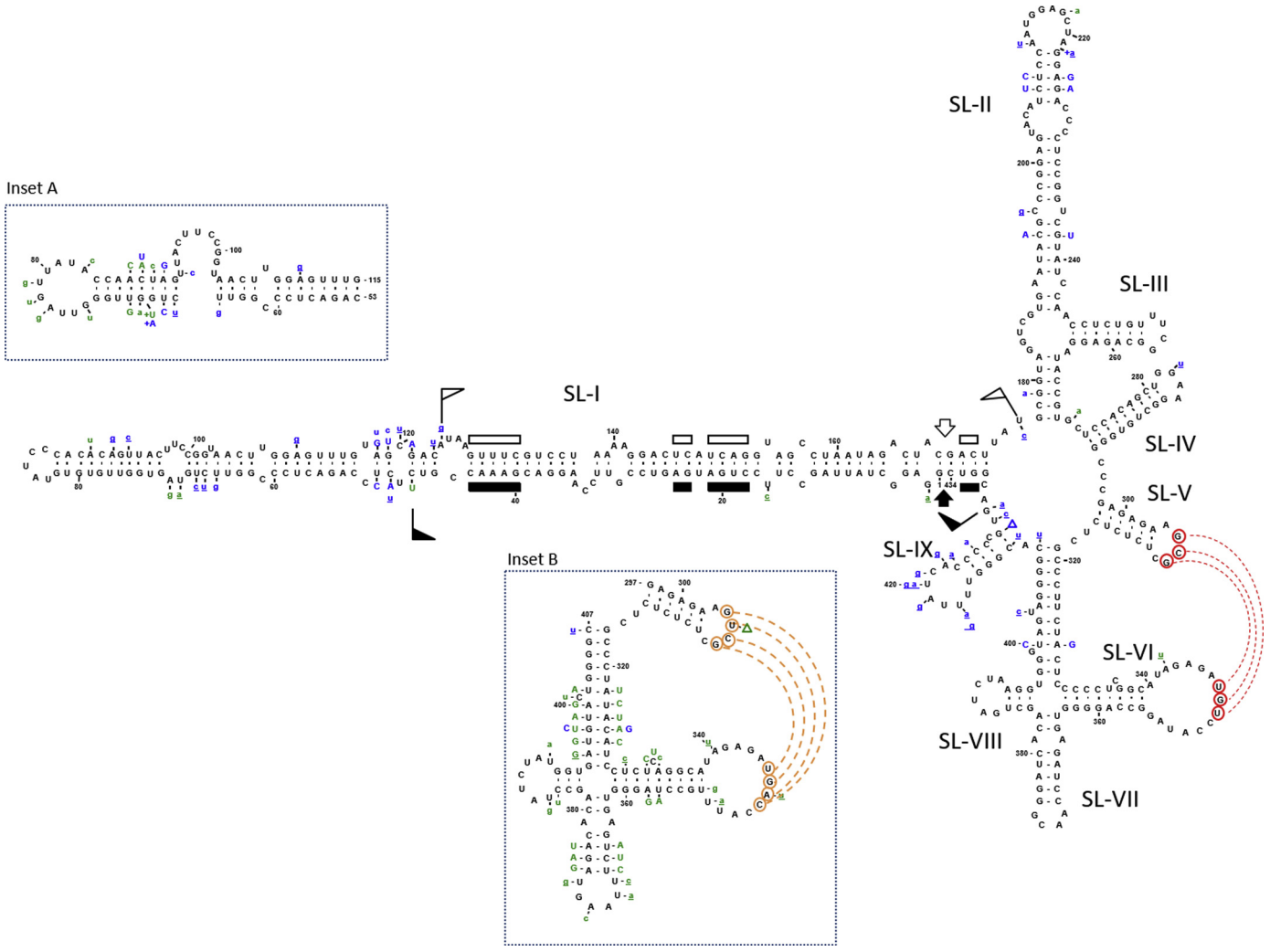

Fig. 4. Primary and predicted secondary structure of the lowest free energy of the AHVd variant AHVd-IT_MRG_01 (MH643712). Flags delimit (+) and (-) hammerhead self-cleaving domains, with the residues conserved in most natural hammerhead structures marked by bars, and the self-cleavage sites indicated by arrows. Solid and open symbols refer to (+) and (-) polarities, respectively. Residues potentially involved in a kissing-loop interaction between positions 305–307 and 347–349 are indicated by circles and broken-red lines. **Inset A and inset B.** Schematic representation of the secondary structure proposed for the a AHVd reference variant from Canada by Serra et al. (2018) in the regions between the positions 53–115 and 297–407, respectively. Mutations found in variants from both AG and MRG isolates are indicated in green. Mutations found only in AG variants are reported in blue. Co-variations are reported in uppercase; conversions of canonical into wobble base-pairs, or *vice versa*, and changes mapping at loops are indicated in underlined lowercase; changes impairing base pairing are in lowercase. To exclude changes potentially induced by the polymerase during the RT-PCR amplification step, only mutation found in more than one clone were reported.

article (Sanderson and Delano, Can. J. Plant Pathol. In press) reported similar, although not identical, results using their own generated AHVd variants.

Funding

This work has been partially funded by the Apulia Regional Project "Progetto Integrato per la Biodiversità – ReGeFruP", PSR II 2007–2013.

GenBank accessions

MH643696-MH643727

Acknowledgments

We wish to thank Giacinto Donvito and Alessandro Italiano for proving technical support while working on the ReCaS infrastructure, Ricardo Flores for critical reading of the manuscript and Pedro Serra for the help in the analyses of the viroid secondary structure.

Appendix A. Supplementary data

Supplementary material related to this article can be found, in the online version, at doi:https://doi.org/10.1016/j.virusres.2019.197644.

References

Barba, M., Hadidi, A., 2017. Application of next-generation sequencing technologies to viroids. In: Hadidi, A., Flores, R., Randles, J.W., Palukaitis, P. (Eds.), Viroids and Satellites. Academic Press-Elsevier, London, UK, pp. 401–412.

Bussière, F., Ouellet, J., Cote, F., Levesque, D., Perreault, J.P., 2000. Mapping in solution shows the peach latent mosaic viroid to possess a new pseudoknot in a complex, branched secondary structure. J. Virol. 74, 2647–2654.

Codoñer, F.M., Daròs, J.A., Sole, R.V., Elena, S.F., 2006. The fittest versus the flattest: experimental confirmation of the quasispecies effect with subviral pathogens. PLoS Pathog. 2, 1187–1193.

De la Peña, M., Navarro, B., Flores, R., 1999. Mapping the molecular determinant of pathogenicity in a hammerhead viroi h mutation rate of a hamm d: a tetraloop within the in vivo branched RNA conformation. Proc. Natl. Acad. cademy of Sciences 96, 9960–9965.

Di Serio, F., Li, S.-F., Pallás, V., Owens, R.A., Randles, J.W., Sano, T., Verhoeven, J.Th.J., Vidalakis, G., Flores, R., 2017. Viroid Taxonomy. In: Hadidi, A., Flores, R., Randles, J., Palukaitis, P. (Eds.), Viroids and Satellites. Academic press, London UK, pp.

135–146.
Di Serio, F., Ambrós, S., Sano, T., Flores, R., Navarro, B., 2018a. Viroid diseases in pome and stone fruit trees and koch's postulates: a critical assessment. VirusesBasel 10.
Di Serio, F., Li, S.F., Matousek, J., Owens, R.A., Pallas, V., Randles, J.W., Sano, T., Verhoeven, J.T.J., Vidalakis, G., Flores, R., Consortium, I.R., 2018b. ICTV virus taxonomy profile: avsunviroidae. J. Gen. Virol. 99, 611–612.
Diener, T.O., 2003. Discovering viroids—a personal perspective. Nat. Rev. Microbiol. 1, 75.
Elena, S.F., Gomez, G., Daros, J.A., 2009. Evolutionary constraints to viroid evolution. Viruses 1, 241–254.
Fadda, Z., Daros, J.A., Flores, R., Duran-Vila, N., 2003. Identification in eggplant of a variant of citrus exocortis viroid (CEVd) with a 96 nucleotide duplication in the right terminal region of the rod-like secondary structure. Virus Res. 97, 145–149.
Flores, R., Hernández, C., de Alba, A.E.M., Darós, J.A., Di Serio, F., 2005. Viroids and viroid-host interactions. Annu. Rev. Phytopathol. 43, 117–139.
Flores, R., Serra, P., Minoia, S., Di Serio, F., Navarro, B., 2012. Viroids: from genotype to phenotype just relying on RNA sequence and structural motifs. Front. Microbiol. 3.
Flores, R., Minoia, S., Carbonell, A., Gisel, A., Delgado, S., Lopez-Carrasco, A., Navarro, B., Di Serio, F., 2015. Viroids, the simplest RNA replicons: how they manipulate their hosts for being propagated and how their hosts react for containing the infection. Virus Res. 209, 136–145.
Flores, R., Di Serio, F., Navarro, B., Owens, R.A., 2017. Viroid pathogenesis. In: Hadidi, A., Flores, R., Randles, J.W., Palukaitis, P. (Eds.), Viroids and Satellites. Academic Press-Elsevier, London, UK, pp. 401–412.
Foissac, X., Svanella-Dumas, L., Gentit, P., Dulucq, M.J., Candresse, T., 2001. Polyvalent detection of fruit tree Trico, Capillo and Foveaviruses by nested RT-PCR using degenerate and inosine containing primers (DOP RT-PCR). Acta Hortic. Regiotect. 550, 37–43.
Gago, S., De la Peña, M., Flores, R., 2005. A kissing-loop interaction in a hammerhead viroid RNA critical for its in vitro folding and in vivo viability. RNA 11, 1073–1083.
Gago, S., Elena, S.F., Flores, R., Sanjuan, R., 2009. Extremely high mutation rate of a hammerhead viroid. Science 323 1308-1308.
Gago-Zachert, S., 2016. Viroids, infectious long non-coding RNAs with autonomous replication. Virus Res. 212, 12–24.
Gomez, G., Pallás, V., 2013. Viroids: a light in the darkness of the lncRNA-directed regulatory networks in plants. New Phytol. 198, 10–15.
Hall, T., 2001. BioEdit Version 5.0. 6. North Carolina State University. Department of Microbiology, Raleigh, North Carolina, pp. 192.
Haseloff, J., Symons, R.H., 1982. Comparative sequence and structure of viroid-like RNAs of two plant viruses. Nucleic Acids Res. 10, 3681–3691.
Hernández, C., Flores, R., 1992. Plus and minus RNAs of peach latent mosaic viroid self-cleave in vitro via hammerhead structures. Proc. Natl. Acad. Sci. U.S.A. 89, 3711–3715.
López-Carrasco, A., Ballesteros, C., Sentandreu, V., Delgado, S., Gago-Zachert, S., Flores, R., Sanjuán, R., 2017. Different rates of spontaneous mutation of chloroplastic and nuclear viroids as determined by high-fidelity ultra-deep sequencing. PLoS Pathog. 13, e1006547. https://doi.org/10.1371/journal.ppat.1006547.
Lorenz, R., Bernhart, S.H., Zu Siederdissen, C.H., Tafer, H., Flamm, C., Stadler, P.F., Hofacker, I.L., 2011. ViennaRNA package 2.0. Algorithms Mol. Biol. 6, 26.
Marais, A., Faure, C., Bergey, B., Candresse, T., 2018. Viral double-stranded RNAs (dsRNAs) from plants: alternative nucleic acid substrates for high-throughput sequencing. In: Pantaleo, V., Chiumenti, M. (Eds.), Viral Metagenomics. Springer, New York, USA, pp. 45–53.
Messmer, A., Sanderson, D., Braun, G., Serra, P., Flores, R., James, D., 2017. Molecular and phylogenetic identification of unique isolates of hammerhead viroid-like RNA from' Pacific Gala' apple (Malus domestica) in Canada. Can. J. Plant Pathol. 39, 342–353.
Muhire, B.M., Varsani, A., Martin, D.P., 2014. SDT: a virus classification tool based on pairwise sequence alignment and identity calculation. PLoS One 9, e108277.
Navarro, B., Flores, R., 1997. Chrysanthemum chlorotic mottle viroid: unusual structural properties of a subgroup of self-cleaving viroids with hammerhead ribozymes. Proc. Natl. Acad. Sci. U.S.A. 94, 11262–11267.
Palukaitis, P., 2014. What has been happening with viroids? Virus Genes 49, 175–184.
Serra, P., Messmer, A., Sanderson, D., James, D., Flores, R., 2018. Apple hammerhead viroid-like RNA is a bona fide viroid: autonomous replication and structural features support its inclusion as a new member in the genus Pelamoviroid. Virus Res. 249, 8–15.
Szostek, S.A., Wright, A., Harper, S., 2018. First report of apple hammerhead viroid in the US, Japan, Italy, Spain, and New Zealand. Plant Dis. 102, 2670.
Thompson, J.D., Gibson, T.J., Higgins, D.G., 2003. Multiple sequence alignment using ClustalW and ClustalX. Curr. Protoc. Bioinformatics. https://doi.org/10.1002/0471250953.bi0203s00. 0, 2.3.1-2.3.22.
Zerbino, D.R., Birney, E., 2008. Velvet: algorithms for de novo short read assembly using de Bruijn graphs. Genome Res. 18, 821–829.
Zhang, Z., Qi, S., Tang, N., Zhang, X., Chen, S., Zhu, P., Ma, L., Cheng, J., Xu, Y., Lu, M., Wang, H., Ding, S.W., Li, S., Wu, Q., 2014. Discovery of replicating circular RNAs by RNA-seq and computational algorithms. PLoS Pathog. 10, e1004553. https://doi.org/10.1371/journal.ppat.1004553.